

## **Part 3: Computational**

## **Chapter 3: DFT investigation of the frontier orbitals as chemical reactivity indicators in the alkene metathesis reaction**

### **3.1 Motivation**

The perturbation theory is one of the fundamental theories in organic chemistry and describes chemical reactivity in terms of frontier orbitals and the charge of the molecules [1],[2]. Energy ( $\Delta E$ ) is defined as “the energy gained and lost when the orbitals of one reactant overlap with those of another” [2]. Reactions are dominated by either frontier orbital interactions or charge interactions as described in the simplified equation [2], with the first term denoting the contribution of the charge and the second term denoting the contribution of the orbital interaction:

$$\Delta E = -\frac{Q_{nuc.} Q_{elec.}}{\epsilon R} + \frac{2(c_{nuc.} c_{elec.} \beta)^2}{E_{HOMO (nuc.)} - E_{LUMO (elec.)}}$$

In frontier orbital interactions the overlap between the HOMO and the LUMO of the reactants dominate the reaction [3]. These reactions are described as soft-soft interactions [4]. Alkene metathesis is an example of such a reaction where the bonding between reactants is the strongest with greater overlap between the HOMO and LUMO [2].

Therefore, after Chauvin [5] expressed the alkene metathesis reaction as a [2+2] cycloaddition reaction, the orbitals became important. Cycloaddition occurs with the formation of “two new  $\sigma$  bonds from the use of  $\pi$  electrons of the reactants” by the overlap of the interacting molecules’ orbitals [6]. Fig. 1 shows three thermal cycloaddition reactions.

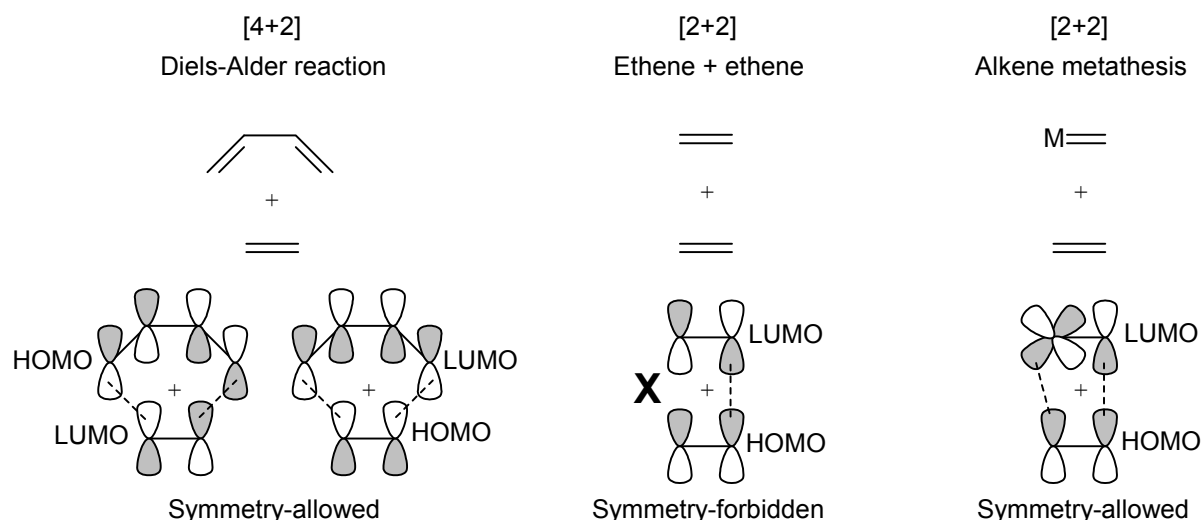


**Fig. 1.** Thermal cycloaddition reactions [6].

The Diels-Alder reaction is a relatively spontaneous concerted reaction, because of the symmetry of the orbitals allowing the same-phase lobes to overlap. The  $[2+2]$  reaction of two ethene molecules is symmetry-forbidden and will only take place in the case of a photochemical reaction [6]. Alkene metathesis on the other hand is a symmetry-allowed  $[2+2]$  cycloaddition reaction, because of the availability of empty d-orbitals of the metal [7],[8].

Other DFT-based chemical reactivity indicators [9] include the Fukui function [10], electronegativity, hardness and softness. A dual descriptor for chemical reactivity, combining the electrophilic and nucleophilic Fukui function as well as the frontier orbitals in one calculation for a point  $\mathbf{r}$ , was also proposed [11-14]. However, Zielinski, Tognetti and Joubert [15] found that the dual descriptor and the Fukui function were in poor agreement and gave conflicting chemical reactivity in some cases. They found Bader's and Hirshfeld's schemes correlated better with their systems [15]. Due to the nature of the alkene metathesis reaction and the modelling software available, we tested only the frontier orbitals as chemical reactivity indicators.

### 3.1.1 References

- [1] F. Jensen, *Introduction to Computational Chemistry*. John Wiley & Sons Inc, Chichester, 2007.
- [2] (a) I. Fleming, *Frontier Orbitals and Organic Chemical Reactions*. WILEY, Chichester, 1976.; (b) I. Fleming, *Molecular Orbitals and Organic Chemical Reactions*, Reference Ed. WILEY, Chichester, 2010.
- [3] T.Clark, *A Handbook of Computational Chemistry: A Practical Guide to Chemical Structure and Energy Calculations*. John Wikey & Sons Inc, New York, 1985.
- [4] G. Klopman, *Chemical Reactivity and Reaction Path*. Wiley, New York, 1974.
- [5] Y. Chauvin, J. Herisson, *Makromol. Chem.* 141 (1971) 161.
- [6] R.T. Morrison, R.N. Boyd, *Organic chemistry*, sixth ed. Prentice Hall International, Inc, New Jersey, 1992.
- [7] T.H. Upton, A.K. Rappé, *J. Am. Chem. Soc.* 107 (1985) 1206.
- [8] F. Mathe, A. Sevin, *Molecular Chemistry of the Transition Elements: An Introductory Course*. John Wiley & Sons, Chichester, 1996.
- [9] H. Chermette, *J.Compt. Chem.* 20 (1999) 129.
- [10] P. Bultinck, S. Fias, C. Van Alsenoy, P.W. Ayers, R. Carbó-Dorca, *J.Chem.Phys.* 127 (2007) 034102.
- [11] C. Morell, A. Grand, A. Toro-Labbé, *J. Phys. Chem. A.* 109 (2005) 205.
- [12] C. Morell, A. Grand, A. Toro-Labbé, *Chem. Phys. Lett.* 425 (2006) 342.
- [13] V. Labet, C. Morell, J. Cadet, L.A. Eriksson, A. Grand, *J. Phys. Chem. A.* 113 (2009) 2524.
- [14] P. Geerlings, P.W. Ayers, A. Toro-Labbé, P.K. Chattaraj, F. De Proft, *Acc. Chem. Res.* 45 (2012) 683.
- [15] F. Zielinski, V. Tognetti, L. Joubert, *Chem. Phys. Lett.* 527 (2012) 67.

## 3.2 Article

### **DFT investigation of the frontier orbitals as chemical reactivity indicators in the alkene metathesis reaction**

#### **Abstract**

The reactivity of metal carbene catalysts in alkene metathesis reactions differs. This has major influences on the efficiency and application of these metal carbenes as metathesis catalysts. The focus of this research is to determine the effectiveness of frontier orbitals as chemical reactivity indicators in the alkene metathesis reaction. Fischer-, Tebbe-, Grubbs-, and Schrock-type metal carbenes were selected. Three elements of the alkene metathesis reaction with these metal carbenes were investigated using computational methods, namely: the generalized trend for alkene metathesis reactivity, the ligand effect on ruthenium metal carbenes and the bonding in the transition state of a Grubbs-type metal carbene catalyzed alkene metathesis reaction. Geometry optimizations of all species were done at the GGA/PW91/DNP level with Materials Studio DMol<sup>3</sup> and subsequent energy calculations were done at B3LYP/LanL2DZ level with Gaussian. The results showed that the frontier orbital interaction of the catalyst-alkene coordination step, for all the major types of metal carbenes, is between the HOMO of the alkene and the LUMO of the catalyst. Furthermore, the location and contribution of atomic orbitals to the LUMO of the metal carbenes can be used as chemical reactivity indicators for the alkene metathesis initiation step and subsequent [2+2] cycloaddition reaction for the formation of the metallacyclobutane intermediate.

#### **Keywords**

Frontier orbitals, alkene metathesis, chemical reactivity, DFT

#### **1. Introduction**

Alkene metathesis is widely used as an important tool in organic synthesis [1]. During alkene metathesis parts of two alkenes are substituted through the breaking and

rearranging of the carbon-carbon double bonds [2]. In 1970 Herrison and Chauvin proposed a metal carbene catalysed mechanism for alkene metathesis [3-5]. The Fischer-type metal carbenes, especially, played a significant role in the eventual acceptance of this mechanism for alkene metathesis reactions [6]. These metal carbenes [6], however, have no to low metathesis reactivity in the self-metathesis of linear alkenes. Decisive experimental support for the metal carbene mechanism came with the discovery of the highly active Schrock- and Grubbs-type metal carbenes [2], based on tungsten or molybdenum and ruthenium respectively [7]. The general mechanism is shown in Fig. 1.

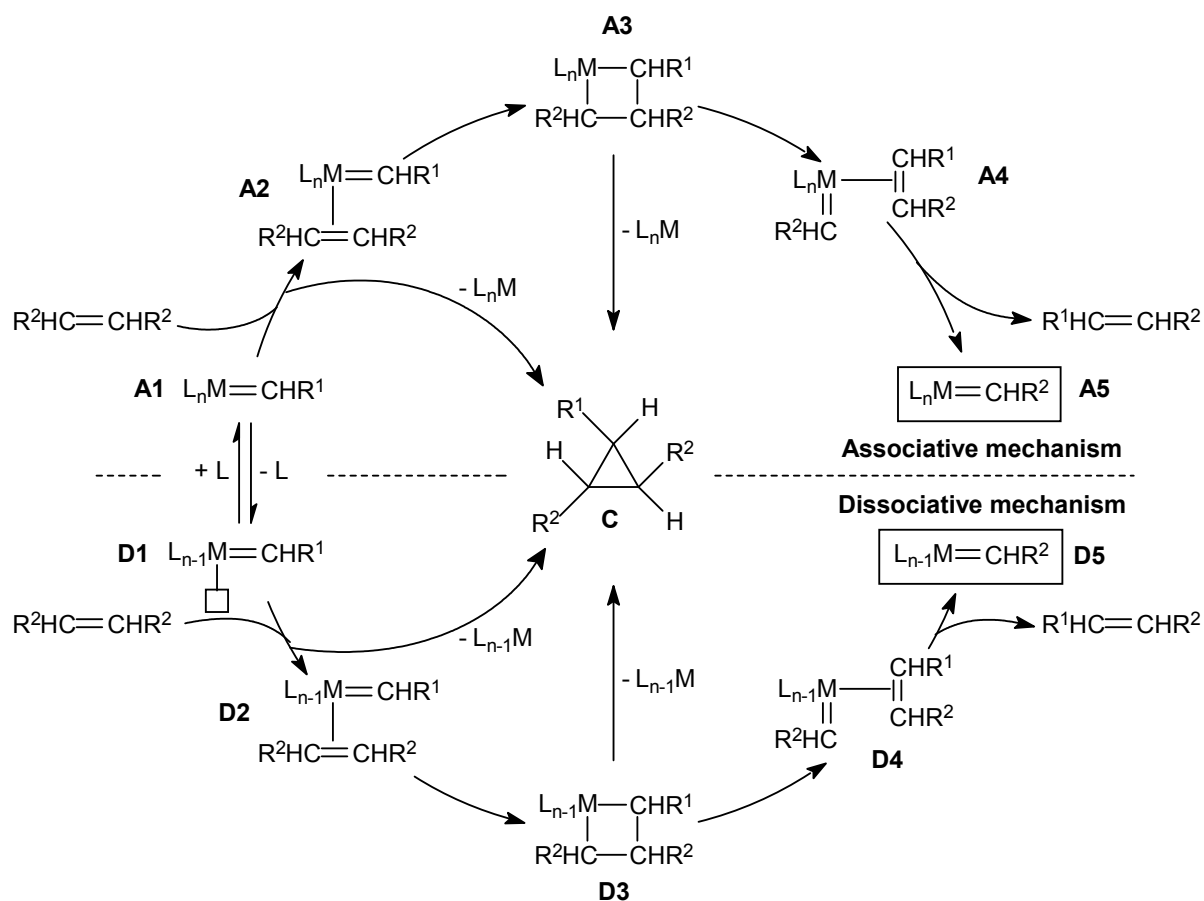


**Fig. 1.** General alkene metathesis mechanisms.

Generally two types of mechanisms are possible. In the associative mechanism the alkene coordinates directly with the metal carbene without dissociation of a ligand, while, in the dissociative mechanism one of the ligands of the metal carbene must first

dissociate before the alkene coordination complex can form. Therefore, in the dissociative mechanism the stable metal carbene acts as a precatalyst and the activated species is the catalyst. Certain metal carbenes, especially Fischer-type metal carbenes, however, form cyclopropane as a major side product of the alkene metathesis reaction as shown in the general mechanism (Fig. 1).

A critical step in the alkene metathesis mechanism is the [2+2] cycloaddition reaction. Cycloaddition reactions result from the overlap between the Highest Occupied Molecular Orbital (HOMO) and the Lowest Unoccupied Molecular Orbital (LUMO) of the reactants [8]. The Woodward-Hoffmann rules state that the [2+2] cycloaddition reaction is forbidden in organic chemistry in the ground state or thermal conditions, but allowed for photochemical processes [3]. However, “calculations on the  $\text{Cl}_2\text{Ti}=\text{CH}_2 + \text{H}_2\text{C}=\text{CH}_2$  system [9] have shown that the presence of the low-energy d-orbitals on the transition metal is sufficient” [10] to allow the reaction under thermal conditions [9].

The major metal carbene types can be arranged according to a generalized trend for the metathesis reactivity for the self-metathesis of linear alkenes (Fig. 2). Both the low oxidation state Fischer carbenes [11], and the high oxidation state Tebbe carbenes [12] have low metathesis reactivity. The high-oxidation-state Grubbs [13] and Schrock [14] carbenes on the other hand have very high metathesis reactivity.

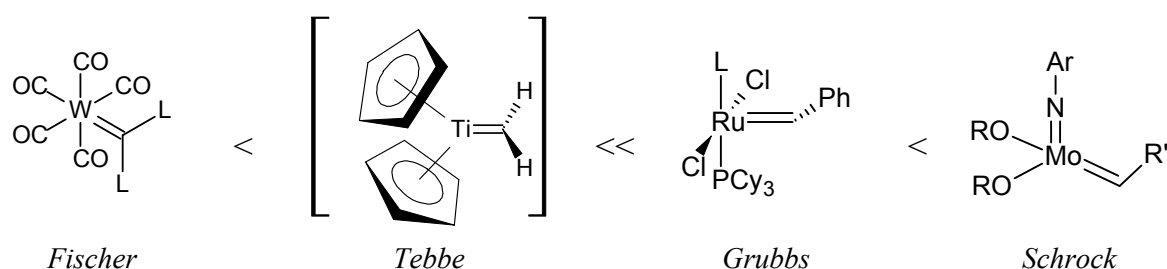


**Fig. 2.** Generalized metathesis reactivity trend of the major metal carbene types.

It is still unclear why only certain metal carbenes show high metathesis reactivity, whereas others show little to no metathesis reactivity. Several computational studies have been done on single metal carbene types, but none on the comparison of the reactivity of the major metal carbene types as defined in Fig. 2. A comparative study done by Occhipinti and Jensen [15] only elucidated the nature of the transition metal-carbene bond with respect to singlet and triplet ground states. Tlenkopatchev and Fomine [16] studied the mechanism by using propene metathesis with a Fischer-type metal carbene catalyst as model reaction. They found that the rate-determining step is the catalyst initiation and stated that the reaction occurs because of the overlap of the HOMO of the alkene with the LUMO of the catalyst located at the carbene carbon. In a study done of the Tebbe-type catalyst Eisenstein and Hoffman [17] did not directly state the use of the frontier orbitals but maintained the importance of the collinear orbital conformation for the formation of the alkene-carbene complex. Suresh and Koga [18] conducted a study on the alkene metathesis of ethene with the model bisphosphine complex  $(\text{PH}_3)_2\text{Ru}(\text{CH}_2)\text{Cl}_2$ . According to them the first transition state for the formation of the metallacyclobutane intermediate is the rate-determining step of the metathesis reaction. They attributed the low barrier of the rate-determining step to two main orbital interactions (a) the strong  $\pi$  orbital interactions between the  $\text{Ru}=\text{CH}_2$  and the alkene moiety in the transition state and (b) the two agostic orbital interactions in the metallacyclobutane. Vyboishchikov, Bühl and Thiel [19] also state that one of the factors necessary for the formation of the alkene-carbene complex are the overlap of the frontier orbitals. On the other hand, Straub [20] shows the active carbene conformation to be the result of the overlap between the bonding orbital of the carbene and the bonding orbital of the alkene which is a high energy interaction. Lord *et al.* [21] investigated the molecular orbital diagram of the metallacyclobutane structure but no mention was made of the initial orbital interaction of the catalyst with the alkene. In a recent study [22] the  $\pi$ - $\pi^*$  attractive interactions through space between a carbon in the NHC-ligand and the carbene carbon were investigated, but again no correlation to the orbital interactions in the complexation step was made. Several other computational studies have also been done on the mechanism of Grubbs-type catalysts [23-36], but none focused on the use of frontier orbitals as



reactivity indicator. Folga and Ziegler [37] did an in-depth study on the possible formations of the molybdenacyclobutane via frontier orbitals. Although not specifically mentioned, they also found the interaction of the alkene HOMO with the catalyst LUMO possible. Fox, Schofield and Schrock [38] came to similar conclusions displaying the overlap of the alkene HOMO with the catalyst LUMO. As a result the general characteristics of the metathesis reaction are well known, but the use of the frontier orbitals as chemical reactivity indicators for all the alkene metathesis reactions, specifically complete catalyst systems, has not yet been widely studied.

In this study three elements of alkene metathesis were investigated using computational methods, namely: the generalized trend for alkene metathesis reactivity, the ligand effect on ruthenium metal carbenes and the bonding in the transition state of a Grubbs-type metal carbene catalyzed alkene metathesis reaction.

To explain the generalized trend for the metathesis reactivity for the self-metathesis of linear alkenes (Fig. 2) of the major metal carbenes, a metal carbene of each type showing metathesis reactivity was selected (Fig. 3), namely: a Fischer-type ((ditoluenecarbene)pentacarbonyltungsten) (**W(Tol)**), the Tebbe reagent (( $\mu$ -Chloro)( $\mu$ -methylene)bis(cyclopentadienyl)(dimethylaluminum)titanium) (**Tebbe**), a Grubbs-type (Grubbs' second-generation catalyst [(H<sub>2</sub>IMes)(PCy<sub>3</sub>)Cl<sub>2</sub>Ru=CHPh]) (**Gr2**) and a Schrock-type (a molybdenum imido alkylidene complex [Mo(CHCMe<sub>2</sub>Ph)(NAr)-[OCMe(CF<sub>3</sub>)<sub>2</sub>]<sub>2</sub>]) (**Mo(Ph)**).

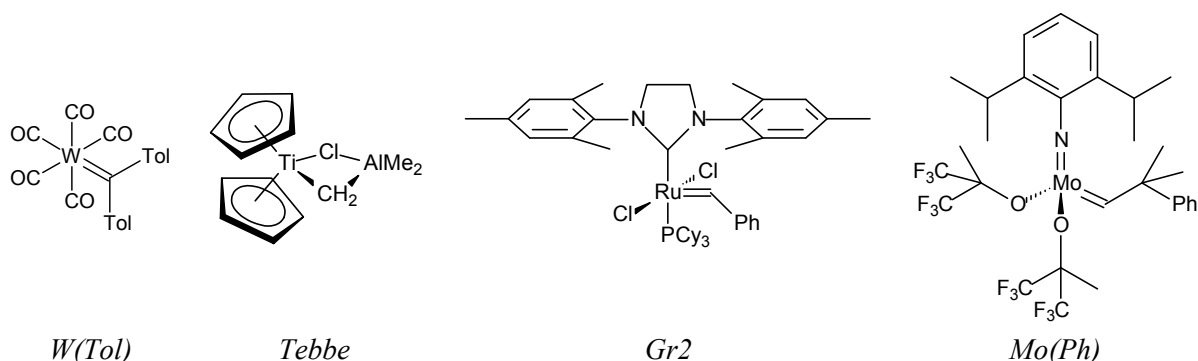


**Fig. 3.** The metal carbenes selected for this study. A Fischer-type (W(Tol)), the Tebbe reagent, a Grubbs-type (Gr2) and a Schrock-type (Mo(Ph)).

The mechanistic steps according to Chauvin's metal carbene catalyzed proposal were studied. It was found experimentally that the selected Fischer [39], Tebbe [12] and Grubbs [40] metal carbenes follow the dissociative mechanism [9],[16],[41-43], whereas the Schrock [14] metal carbene follows the associative mechanism [44],[45]. In the catalyst initiation step a CO-ligand dissociates from **W(Tol)**, the AlClMe<sub>2</sub>-ligand dissociates from the **Tebbe** reagent and the PCy<sub>3</sub>-ligand dissociates from **Gr2**.

For the dissociative mechanism there is a catalyst initiation step to activate the precatalyst (**pre**) for metathesis. In the catalyst coordination step the alkene coordinates to the metal atom of the catalyst (**cat**), before forming the metallacyclobutane intermediate. Therefore the proposed active site on which we will focus in this study is the metal atom of the catalyst. We will investigate the nature of the frontier orbitals at the active site and also the contribution of the different atoms of the catalytic species to the frontier orbitals.

## 2. Computational methods

Five software programs were used for the molecular modeling, namely: Accelrys Materials Studio 5.0 [46] and Gaussian 03 [47] for the calculations, and Chemission [48], GaussView [49] and Solid Angle [50] for the visualizations.

The initial geometry optimization calculations of all the species, and the potential energy surface (PES) scans, were done with DMol<sup>3</sup> a DFT module of Accelrys Materials Studio 5.0. The GGA PW91 functional with the DNP basis set was used. To calculate the transition state of the reaction of ethene with **Gr2**, a potential-energy surface (PES) scan of the metallacyclobutane intermediate was done. The scan was done by lengthening the carbon-carbon bond between the carbene carbon and the alkene carbon not bonded to the ruthenium atom stepwise (Fig. 4) (See Appendix A Fig. A.1 for the input file of the PES scan).

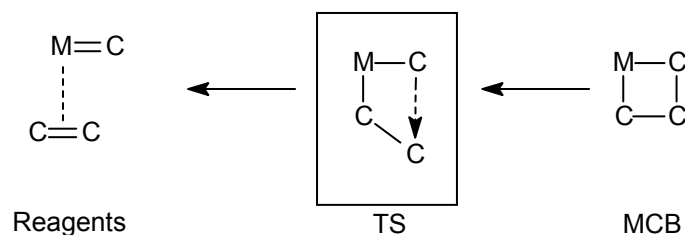


**Fig. 4.** The C-C bond of the metallacyclobutane intermediate lengthened for the calculation of the potential-energy surface scan.

A frequency calculation was then run of the highest-energy structure to determine whether there is only one imaginary frequency and thus a true transition-state structure was obtained. A further transition-state optimization with DMol<sup>3</sup> was also done to gain the optimum transition state. However, no orbital calculations were done with Materials Studio, because it is not possible to retrieve the coefficients of the contribution of the various AOs to the molecular orbitals (MO) from Accelrys Materials Studio.

The Accelrys Materials Studio geometry optimized structures were imported into Gaussian 03 and used as starting structures in the single-point-energy calculation to obtain the population of the orbitals. The B3LYP functional and LanL2DZ basis set in Gaussian were used for the calculations as it is widely used for organometallic calculations. Furthermore, the chosen PW91 functional in DMol<sup>3</sup> is unavailable in Gaussian. In order to access the coefficients from the output file, the following route line was used in Gaussian: #P (method)(basis set) pop=full GFInput.

Chemission, a tool for the analysis of the electronic structure of molecules [48], was used to retrieve the coefficients from the Gaussian output file (.out). GaussView [49] was used to visualize the MOs. The surface was drawn with a default isovalue of 0.02. By Z-clipping the surface of the MOs in GaussView and exporting the resulting image to graphical drawing software, i.e. Coral Draw, the atomic orbitals could be overlaid on the MOs.

For the investigation of the availability of the metal atom for coordination Solid-G was used. Solid-G is a software program designed to calculate a number of geometrical parameters for ligand coordination to metal complexes [50]. For this study the GM(complex) value was calculated. The GM(complex) value is the percentage of the metal M coordination sphere shielded by all ligands [50].

### 3. Results and Discussion

#### 3.1 Generalized trend of alkene metathesis reactivity

According to the Frontier Molecular Orbital (FMO) theory, bonding between reactants is strongest with greater overlap between the HOMO and LUMO [51]. The locations of the LUMO and HOMO indicate the sites of a nucleophilic or electrophilic attack. A nucleophile with a relatively high energy HOMO, will react with an electrophile with a relatively low energy LUMO [51],[52]. Thus, to determine which frontier orbitals overlap for the formation of the coordinated alkene-catalyst-complex the absolute difference between the energy of the HOMO ( $E_{\text{HOMO}}$ ) and the energy of the LUMO ( $E_{\text{LUMO}}$ ) was calculated (Table 1).

**Table 1** Frontier orbital overlaps of the four types of metal carbenes with 1-pentene

|                   | $E_{\text{HOMO}}$<br>(eV) | $E_{\text{LUMO}}$<br>(eV) | $ E_{\text{HOMO(catalyst)}} - E_{\text{LUMO(alkene)}} $ | $ E_{\text{HOMO(alkene)}} - E_{\text{LUMO(catalyst)}} $ |
|-------------------|---------------------------|---------------------------|---|---|
| <i>W(Tol)_cat</i> | -5.0                      | -3.8                      | 4.8   | 2.1   |
| <i>Tebbe_cat</i>  | -4.5                      | -2.9                      | 4.3   | 3.1   |
| <i>Gr2_cat</i>    | -4.5                      | -3.3                      | 4.3   | 2.6   |
| <i>Mo(Ph)</i>     | -5.7                      | -3.4                      | 5.5   | 2.5   |
| $C_5$             | -5.9                      | -0.2                      |   |   |

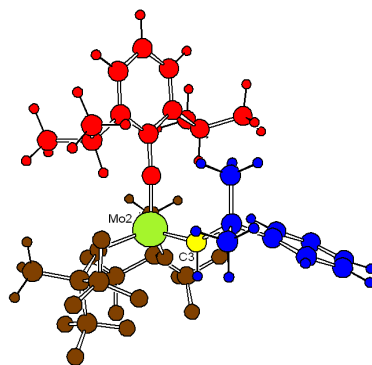
This was first done for the HOMO of the catalyst and the LUMO of the alkene and then for the HOMO of the alkene and the LUMO of the catalyst. For the frontier-orbital-energy gap calculation 1-pentene ( $C_5$ ) was used. This was done because experimental results for the self-metathesis of a linear alkene with a Fischer-type metal carbene are available for the reaction of 1-pentene.[39] The frontier orbital

overlaps of the four types of metal carbenes with  $C_5$  (Table 1) indicated that in all four cases the smallest HOMO-LUMO energy gap i.e.  $|\Delta E|$ , is between the HOMO of the alkene and the LUMO of the metal carbene. This supports the results of Tlenkopatchev and Fomine [16] for the Fischer-type carbene and the statements made for the Schrock-type carbene [37],[38]. Thus according to FMO theory, based on the energy-gap values the general reactivity towards alkenes is expected to be **Tebbe\_cat** < **Gr2\_cat** < **Mo(Ph)** < **W(Tol)\_cat** [53]. However, in the case of Fischer metal carbenes the major product is cyclopropane [5],[39],[54-60] and little to no metathesis products are formed. For the formation of cyclopropane the alkene has to coordinate to the carbene carbon atom, [5] whereas for metathesis product formation the alkene coordinates at the metal atom of the carbene [3-5]. Thus, if **W(Tol)\_cat** is left out and only metathesis reactivity is considered, the reactivity trend matches the generalized reactivity trend for self-metathesis of linear alkenes (Fig. 2). Based on the above,  $E_{LUMO}$  of the catalyst can be considered in combination with the location of the LUMO. The latter could influence the product distribution, as is observed in Fischer carbenes forming a cyclopropane group [53].

In order to prove the reliability of the LUMO frontier orbital as chemical reactivity indicator for the alkene metathesis catalyst, the catalyst initiation step was investigated. Initiation takes place when one of the  $PCy_3$ -ligands dissociates from the precatalyst (**A1** in Fig. 1) to produce the catalytic active species (**D1** in Fig. 1). This was done by calculating the percentage AO coefficient contributions of each part of the molecule to the LUMO MOs of the precatalyst and catalyst species. For this purpose Chemission was used. In the case of Fischer-, Tebbe- and Grubbs-type metal carbenes that follow the dissociative mechanism the precatalyst and catalyst species were calculated. However, for the Schrock-type metal carbene only the precatalyst species was calculated according to the associative mechanism. The molecular fragmentation of each species was configured by defining the groups of atoms that form each part of the molecule (Fig. 5). This allowed a comparison of the contribution of the corresponding fragments across the four types of metal carbenes. The AO

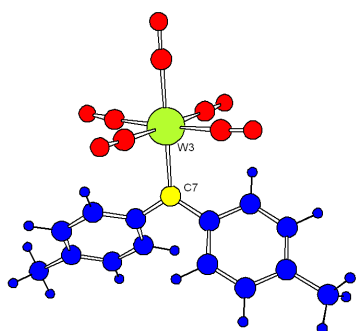
coefficient, and contributions of each fragment to the LUMO of the catalyst, were then calculated using Chemissian and the results are presented as pie charts (Fig. 6).

*Associative: Mo(Ph)*

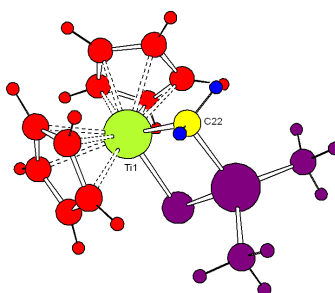


*Mo(Ph)*

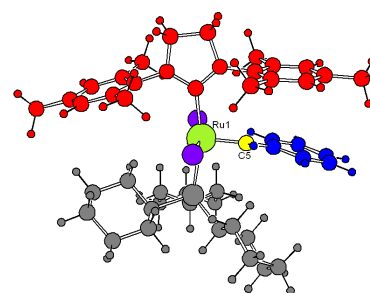
*Dissociative: W(Tol), Tebbe and Gr2*



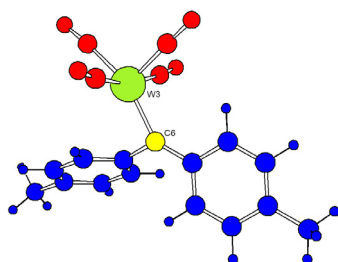
*W(Tol)\_pre*



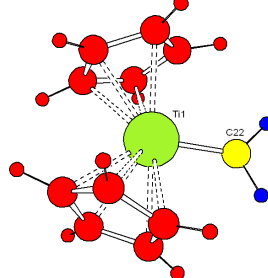
*Tebbe\_pre*



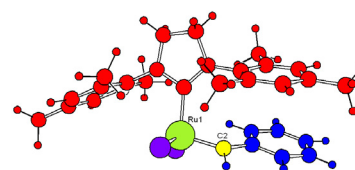
*Gr2\_pre*



*W(Tol)\_cat*



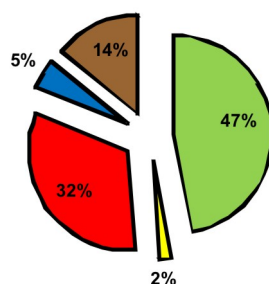
*Tebbe\_cat*



*Gr2\_cat*

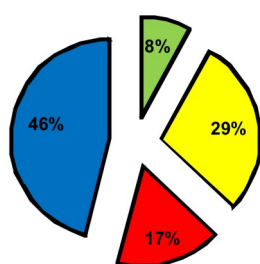
**Fig. 5.** The defined fragmentation of the catalytic species. The fragments for each species were defined according to the following, namely: a top ligand (red), the metal atom (green), the carbene carbon (yellow), the carbene carbon substituent (blue). For **Gr2** the additional fragments are the chlorine ligands (purple) and the PCy<sub>3</sub>-ligand (grey). In the Tebbe reagent the AlCIME<sub>2</sub>-ligand is purple and in the **Mo(Ph)** catalyst the [OCMe(CF<sub>3</sub>)<sub>2</sub>]<sub>2</sub>-ligands are brown.

*Associative: Mo(Ph)*

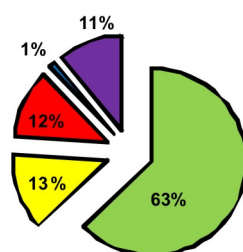


*Mo(Ph)*

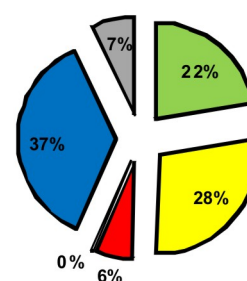
*Dissociative: W(Tol), Tebbe and Gr2*



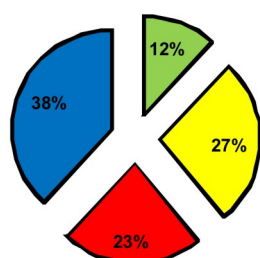
*W(Tol)\_pre*



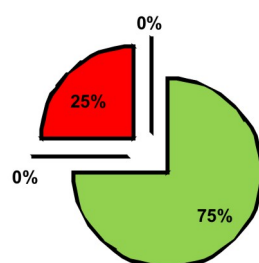
*Tebbe\_pre*



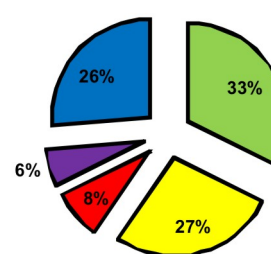
*Gr2\_pre*



*W(Tol)\_cat*



*Tebbe\_cat*



*Gr2\_cat*

**Fig. 6.** Contribution of each fragment to the LUMO of the catalytic species.

A possible explanation why the **Mo(Ph)** catalyst follows the associative mechanism is because the contribution of the molybdenum atom is 47% without dissociation of a ligand with the contribution of the carbene carbon only 2%. This may be an explanation for the high metathesis reactivity of **Mo(Ph)** [14], because the HOMO of the alkene will selectively coordinate to the molybdenum atom rather than the carbene

carbon atom preventing the formation of cyclopropane. On the other hand, cyclopropane is one of the major products formed in the reaction of an alkene with **W(Tol)**. This is seen in Fig. 6 where the tungsten contributes only 8% of the LUMO in **W(Tol)\_pre**, changing to only 12% after dissociation of the CO-ligand, whereas the carbene carbon contributes 29% in **W(Tol)\_pre** and 27% in **W(Tol)\_cat**. There is a clear indication that the carbene carbon will be the selected site of coordination of the alkene. In both the **Tebbe\_pre** and **Tebbe\_cat** species the contribution of the titanium atom is very high, namely 63% and 75%. The alkene should coordinate only at the metal atom. However, from the literature [12] we know that the Tebbe reagent is not a very active alkene metathesis catalyst, thus the higher energy of the LUMO or stereochemical factors effectively act as a barrier to higher metathesis reactivity. For **Gr2** the change in percentage contribution of the Ru atom, from 22% to 33% after dissociation of the PCy<sub>3</sub>-ligand, confirms the greater accessibility of the Ru atom for coordination of an alkene and thus the need for a dissociation step.

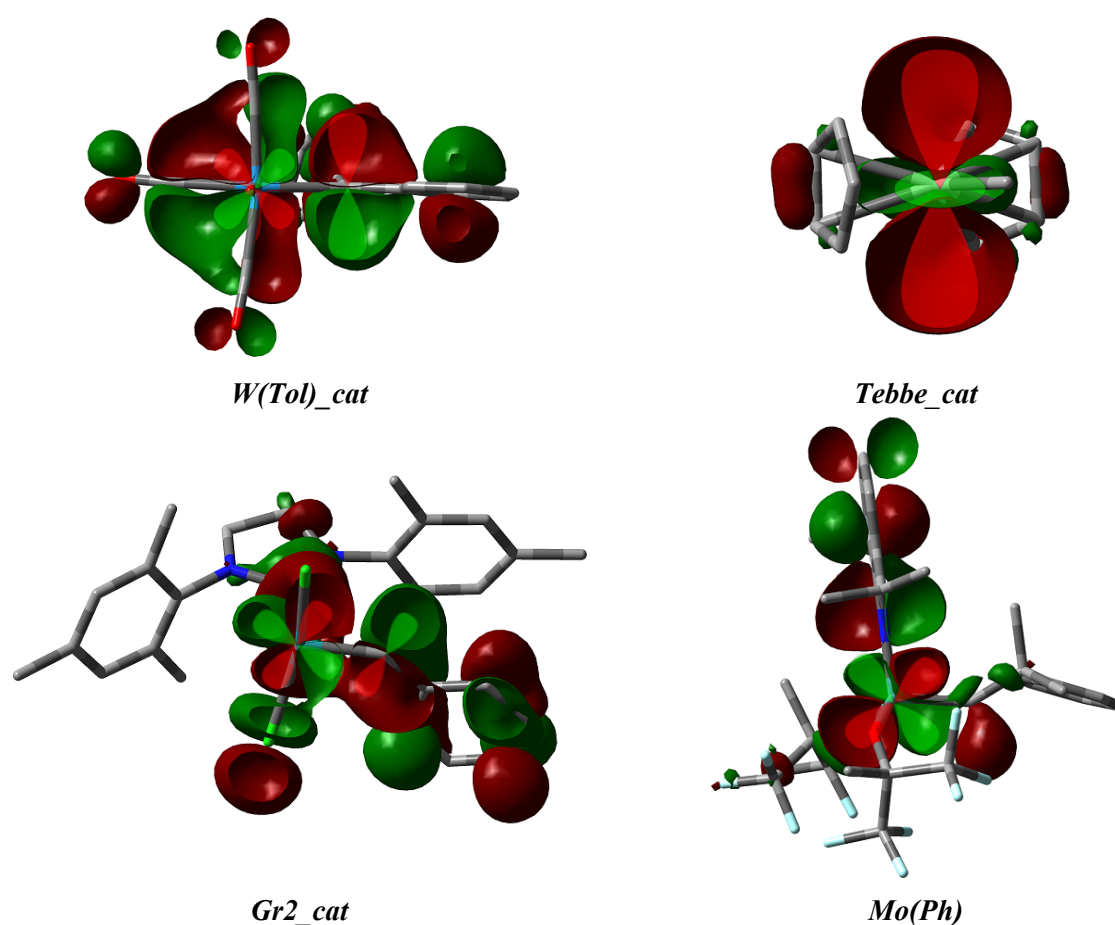
The next step was a more in-depth investigation into the specific atomic orbital (AO) coefficients contributing to the LUMO of each catalytic species. The values of the coefficients range from -1 to +1. For the purpose of this study only coefficients between -1 to -0.2 and 0.2 to 1 were considered, because the focus is only on the major contributors to the MOs. Furthermore, only the coefficients of the metal atom, the carbene carbon atom and the carbon atoms of the coordinated alkene were investigated. Thus, for each catalyst the coefficients of the metal atom and the carbene carbon atom, with an absolute value of greater than 0.2, were calculated (Table 2).

**Table 2** |Orbital coefficients| >0.2 of the AO of the metal to the LUMO of the catalyst

| <i>W(Tol)_cat</i> |                 |             | <i>Tebbe_cat</i> |  |             | <i>Gr2_cat</i> |                 |             | <i>Mo(Ph)</i> |                 |             |
|-------------------|-----------------|-------------|------------------|--|-------------|----------------|-----------------|-------------|---------------|-----------------|-------------|
| Atom              | AO              | coefficient | Atom             | AO                                       | coefficient | Atom           | AO              | coefficient | Atom          | AO              | coefficient |
| C 6               | p <sub>z</sub>  | 0.45        | Ti 1             | d <sub>z<sup>2</sup>-r<sup>2</sup></sub> | 0.72        | Ru 1           | d <sub>xy</sub> | 0.44        | Mo 2          | d <sub>xy</sub> | 0.5         |
| C 6               | p <sub>z</sub>  | 0.28        | Ti 1             | d <sub>z<sup>2</sup>-r<sup>2</sup></sub> | 0.28        | C 2            | p <sub>y</sub>  | 0.37        | Mo 2          | d <sub>yz</sub> | 0.35        |
| W 3               | d <sub>xz</sub> | 0.21        |                  |  |             | C 2            | p <sub>y</sub>  | 0.26        | Mo 2          | d <sub>xz</sub> | 0.33        |
|                   |                 |             |                  |  |             | Ru 1           | d <sub>yz</sub> | 0.21        |               |                 |             |

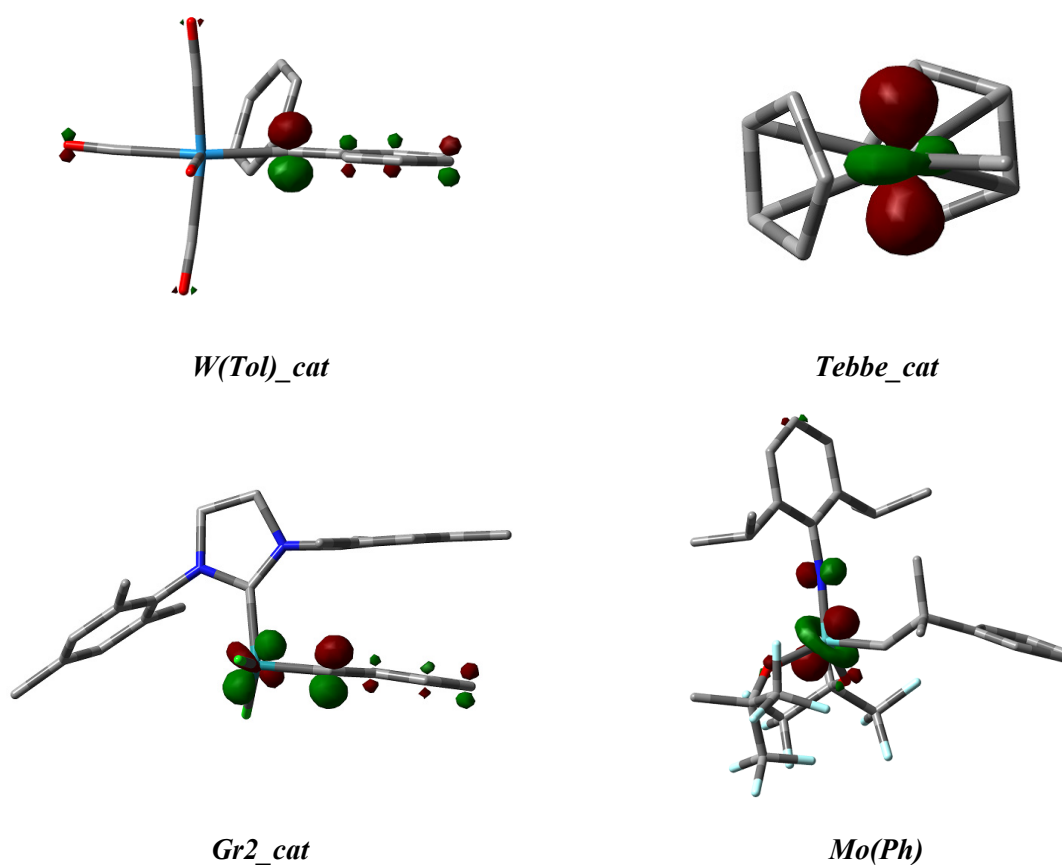


The AOs are named according to an internal standard Cartesian axes defined by Gaussian for each calculated molecule. For **W(Tol)\_cat** the biggest coefficient of the metal carbene is the  $p_z$ -orbital (0.45) of the carbon, with the tungsten  $d_{xz}$ -orbital coefficient only 0.21. This further confirms the carbene carbon as the selected site for an alkene coordination in **W(Tol)\_cat**. In the case of the **Tebbe\_cat**, **Gr2\_cat** and the **Mo(Ph)** the biggest AO coefficient is on the metal atom. For the **Tebbe\_cat** it is the  $d_{z^2}$ -orbital (0.72), and in both the **Gr2\_cat** and **Mo(Ph)** it is the  $d_{xy}$ -orbital (respectively 0.44 and 0.50). The coefficients confirm the metal as the probable site for an alkene coordination in the **Tebbe\_cat**, **Gr2\_cat** and **Mo(Ph)**. If we make a cut through the LUMO surface of each catalyst (Fig. 7), we can see the contribution of each AO to the LUMO. It is clear that the contribution to the LUMO of the metal and carbene carbon comes from the AOs on the two atoms.

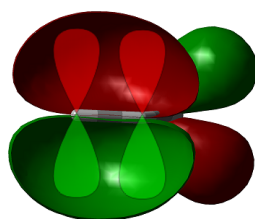


**Fig. 7.** Overlay of the AOs of the metal and carbene carbon atom on the LUMO.

This is confirmed by drawing the LUMO surface with an isovalue of 0.1 (Fig. 8). Thus for simplification only the AOs are used for the possible bonding overlap for the formation of the alkene-metal-complex. 1-Pentene was again used as alkene to show the possible overlap of the catalyst with the alkene. The AO coefficients on the carbon atoms of the double bond are  $p_z(0.49)$  and  $p_z(0.49)$  respectively. Fig. 9 shows the overlay of the AOs on the HOMO of 1-pentene.



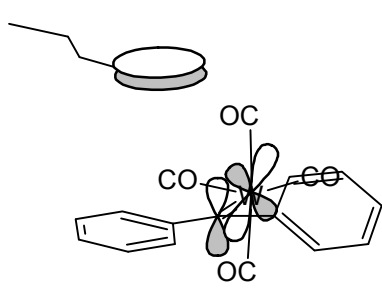
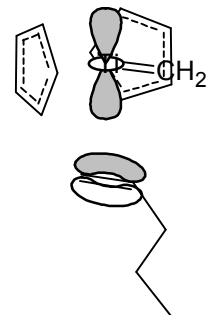
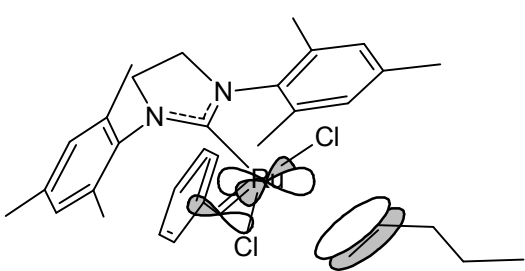
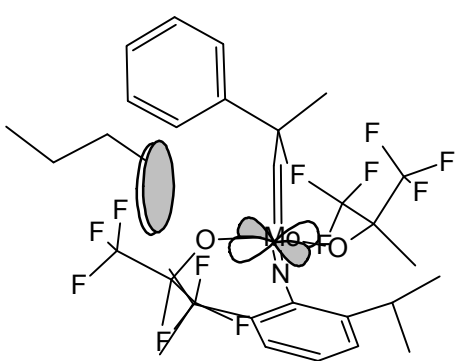
**Fig. 8.** The LUMO surfaces of the catalysts with an isovalue set to 0.1.



**Fig. 9.** Overlay of AO on HOMO of pentene.

The orientation of the d-orbitals gives a further insight into the difference in reactivity of the catalysts. Depending on the orientation of the alkene and the accessibility to the metal atom, the orientation of the d-orbitals has an effect on the possible overlap of the frontier orbitals and the resulting product formation [10]. In Table 3 the possible orbital overlaps are shown for the biggest coefficients of each MO. For **W(Tol)\_cat** the biggest overlap is between the carbene carbon and the alkene confirming the formation of cyclopropane. In the **Tebbe\_cat** there is overlap possible between the alkene and the metal atom, but there is no coefficient on the carbene carbon. For metathesis products to form there must be a [2+2] cycloaddition reaction. This is not possible for the **Tebbe\_cat**, because there is no contribution from the carbene carbon. In both the **Gr2\_cat** and **Mo(Ph)** the one alkene carbon coordinates to the metal atom first with secondary overlap possible at the carbene carbon for the formation of the metallacyclobutane intermediate via [2+2] cycloaddition.

**Table 3** Possible orbital overlaps with coefficients in brackets

| <i>W(Tol)_cat</i> (LUMO) and alkene(HOMO)  |                             | <i>Tebbe_cat</i> (LUMO) and alkene(HOMO)  |                             |
|--|-----------------------------|---|-----------------------------|
| $W_{\text{cat}} d_{xz}$ (0.21)   | $C_{\text{cat}} p_z$ (0.45) | $Ti_{\text{cat}} d_{z^2-f}^2$ (0.72)  | $C_{\text{cat}} p_z$ (0)    |
|   |                             |  |                             |
| $C_{\text{alk}} p_z$ (0.49)  | $C_{\text{alk}} p_z$ (0.49) | $C_{\text{alk}} p_z$ (0.49)   | $C_{\text{alk}} p_z$ (0.49) |
| <i>Gr2_cat</i> (LUMO) and alkene(HOMO)   |                             | <i>Mo(Ph)</i> (LUMO) and alkene(HOMO)   |                             |
| $Ru_{\text{cat}} d_{xy}$ (0.44)  | $C_{\text{cat}} p_y$ (0.37) | $Mo_{\text{cat}} d_{xy}$ (0.50)   | $C_{\text{cat}} p_z$ (0.12) |
|  |                             |  |                             |
| $C_{\text{alk}} p_z$ (0.49)  | $C_{\text{alk}} p_z$ (0.49) | $C_{\text{alk}} p_z$ (0.49)   | $C_{\text{alk}} p_z$ (0.49) |

For the coordination of the alkene with the metal atom to take place, the metal atom must be accessible to the alkene. This accessibility was calculated with Solid-G (Fig. 10). In the figure each catalyst is portrayed as a sphere, with the central atom the metal atom. The aim of the sphere is to show the shielding of the metal atom by the ligands. This is done by defining the shadow of the ligand on the outer surface of the sphere. The open space is then the space where possible coordination with an alkene can take place. G(complex) percentage values are then given for the amount of shielding by the ligands. Results show that the metal atom of **W(Tol)\_cat** and **Tebbe\_cat** is significantly shielded by the ligands (81% and 79% respectively). The metal atom of **Mo(Ph)** is slightly more accessible (77% shielding), with the **Gr2\_cat** metal atom the most accessible (only 65% shielding).

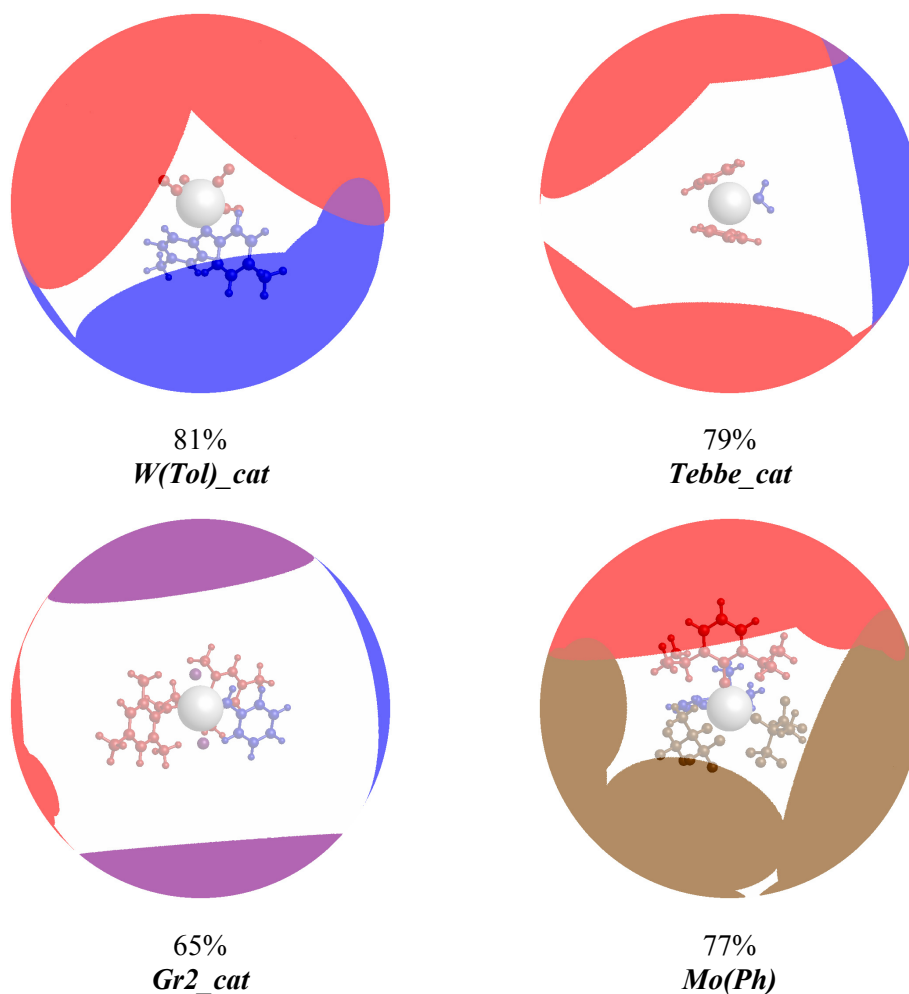


**Fig. 10.** The percentage shielding of the metal atom by the ligands ( $G(\text{complex})$  values) [34].

### 3.2 Ligand effect

From the results of the investigation of the generalized trend for the reactivity of alkene metathesis catalysts it is clear that the energy, MO contribution coefficients and AO orientation of the LUMO of the catalysts can possibly act as chemical reactivity indicators for the alkene metathesis mechanism. Thus, to understand further the reactivity of a metal carbene for alkene metathesis we looked at the effect of the ligands. What would be the effect of a change in ligands on the energy, MO coefficients and AO orientation of the LUMO of the catalyst [50]? For this purpose we investigated a series of active ruthenium metal carbenes, namely: benzylidene-dichloro(bis(tricyclohexyl-phosphine))ruthenium (**Gr1**), **Gr2** and indenylidene-

dichloro(tricyclohexyl-phosphine)(1,3-bis-(2,4,6-trimethylphenyl)-2-imadazolidinylidene)-ruthenium (**Gr2\_indy**) [61]. Additionally a simplified model of the ruthenium metal carbene,  $\text{H}_3\text{Ru}=\text{CH}_2$  (**Ru(H)**), was calculated. The active species after dissociation of a ligand were investigated, because all three active catalysts follow the dissociative mechanism [6]. For each species the fragments were defined as was the case for **Gr2\_cat** in Fig. 4 (Fig. 11). The top ligand is red, the metal atom is green, the carbene carbon is yellow, the carbene carbon substituent is blue and in the case of **Gr1\_cat**, **Gr2\_cat** and **Gr2\_indy\_cat** the chlorine ligands are purple. We chose **Gr2\_cat** as the control. If we change the top ligand we get **Gr1\_cat**, if we change the carbene carbon substituent we get **Gr2\_indy\_cat** and if we change all the ligands to hydrogen atoms we get **Ru(H)**.

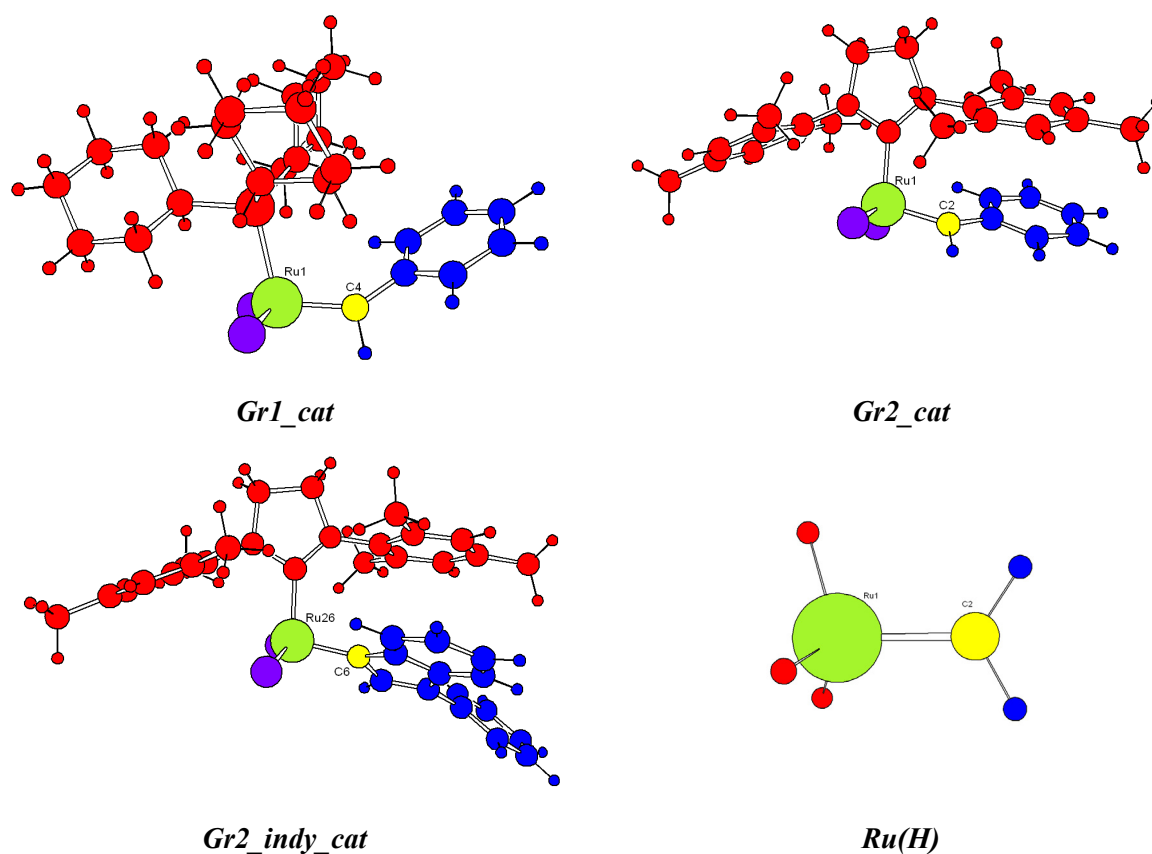


**Fig. 11.** Key to the fragmentation of each molecule as defined in the pie charts.

For all four the ruthenium metal carbenes the biggest contribution to the LUMO of the molecule (Fig. 12) is from the ruthenium atom. If the top ligand changes from H<sub>2</sub>IMes to PCy<sub>3</sub> (**Gr1\_cat**) there is a percentage rise on the ruthenium atom of 8%. If the carbene carbon ligand is changed from benzylidene to indenylidene (**Gr2\_indy\_cat**) there is a percentage drop of 3% on the ruthenium atom and if all the ligands of **Gr2\_cat** are changed to hydrogens (**Ru(H)**) the percentage doubles on the ruthenium atom. The energy of the LUMO of the molecules increases in the order **Ru(H)**< **Gr2\_indy\_cat**< **Gr2\_cat**< **Gr1\_cat**.

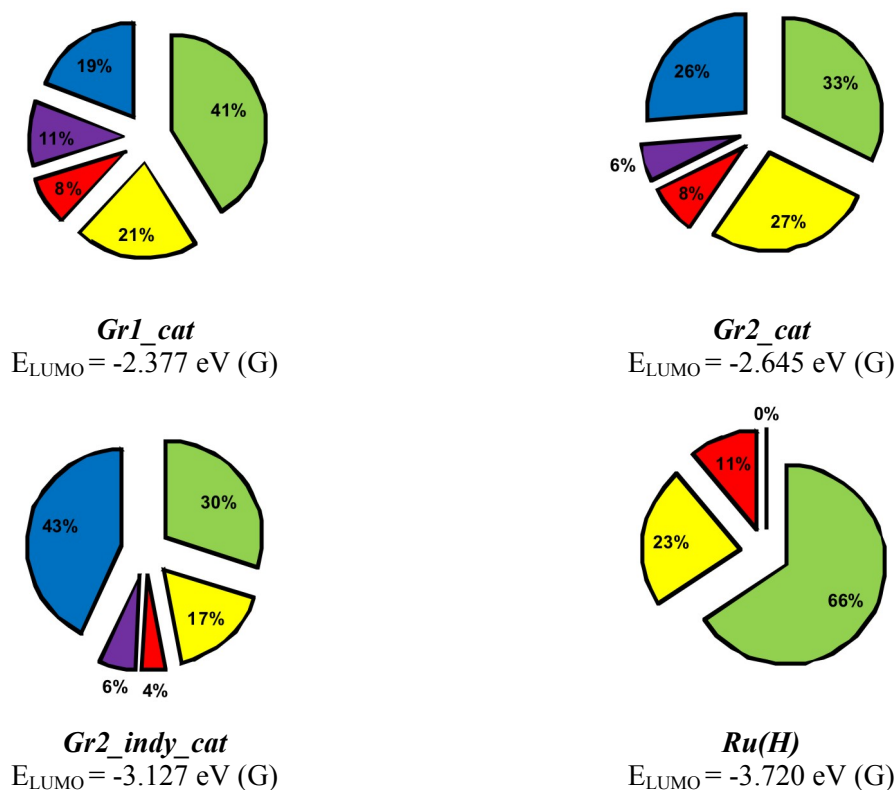


**Fig. 12.** Contribution of each fragment to the LUMO of the molecule.

The MO contribution coefficients of **Gr2\_cat**, also undergo a change if the ligands are changed. A change in the top ligand (**Gr1\_cat**) causes a 0.05 drop in the Ru AO coefficient ( $d_{xy}$ ). If on the other hand the carbene carbon ligand is changed (**Gr2\_indy\_cat**) the Ru AO coefficient drops 0.08 ( $d_{xz}$ ). In the case of **Ru(H)** the Ru AO coefficient rises with 0.03 ( $d_{yz}$ ) (Table 4).

**Table 4** |Orbital coefficients| >0.2 of the AO of the metal to the LUMO of the molecule

| <i>Gr1_cat</i> |               |                  | <i>Gr2_cat</i> |          |                  | <i>Gr2_indy_cat</i> |          |                  | <i>Ru(H)</i> |               |                  |
|----------------|---------------|------------------|----------------|----------|------------------|---------------------|----------|------------------|--------------|---------------|------------------|
| Atom           | AO            | coef-<br>ficient | Atom           | AO       | coef-<br>ficient | Atom                | AO       | coef-<br>ficient | Atom         | AO            | coef-<br>ficient |
| Ru 1           | $d_{xy}$      | 0.39             | Ru 1           | $d_{xy}$ | 0.44             | Ru 26               | $d_{xz}$ | 0.36             | Ru 1         | $d_{yz}$      | 0.47             |
| C 4            | $p_z$         | 0.30             | C 2            | $p_y$    | 0.37             | C 6                 | $p_z$    | 0.27             | C 2          | $p_z$         | 0.33             |
| Ru 1           | $d_{xz}$      | 0.29             | C 2            | $p_y$    | 0.26             | Ru 26               | $d_{yz}$ | 0.24             | Ru 1         | $d_{z^2-r^2}$ | 0.23             |
| Ru 1           | $d_{yz}$      | 0.27             | Ru 1           | $d_{yz}$ | 0.21             | C 6                 | $p_y$    | 0.21             | C 2          | $p_z$         | 0.22             |
| C 4            | $p_z$         | 0.26             |                |          |                  | Ru 26               | $d_{xy}$ | 0.20             |              |               |                  |
| C 4            | $p_y$         | 0.23             |                |          |                  |                     |          |                  |              |               |                  |
| Ru 1           | $d_{z^2-r^2}$ | 0.22             |                |          |                  |                     |          |                  |              |               |                  |

The overlay of the AOs of the metal and carbene carbon atom on the LUMOs is shown in Fig. 13. It is shown that the AOs can again be used as a prediction for the overlap between the alkene and the catalyst, because of the good correlation of the relative size and position with the LUMOs.

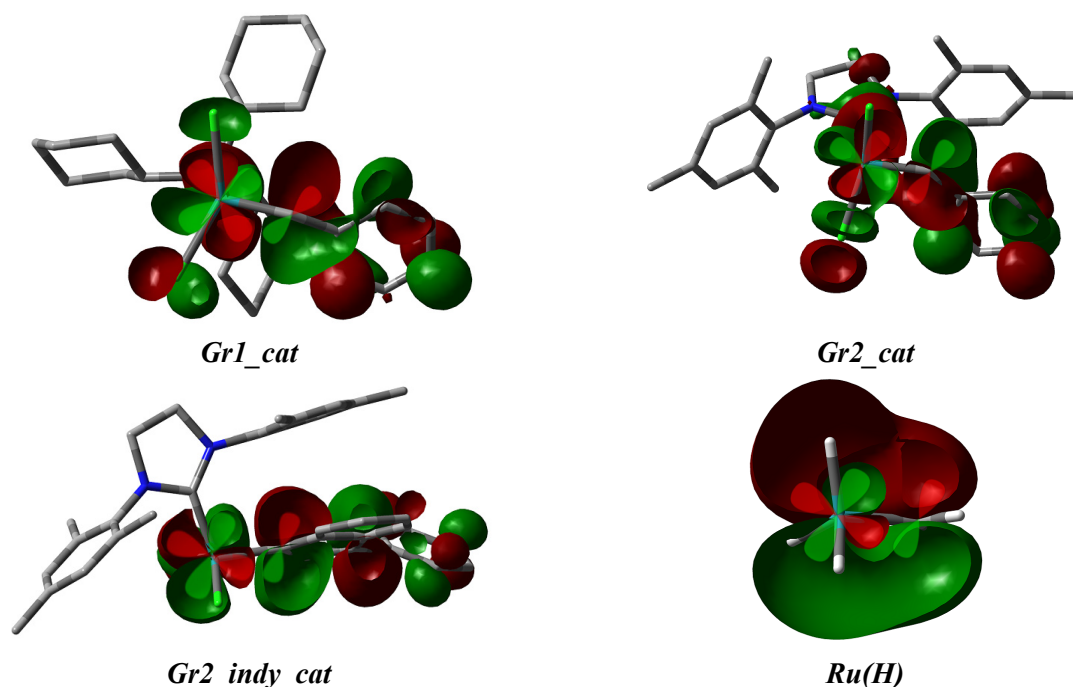


**Fig. 13.** Overlay of AOs of the metal and carbene carbon atom on the LUMO.



This is again confirmed by the MO surface drawings with the isovalue set to 0.1 (Fig. 14).

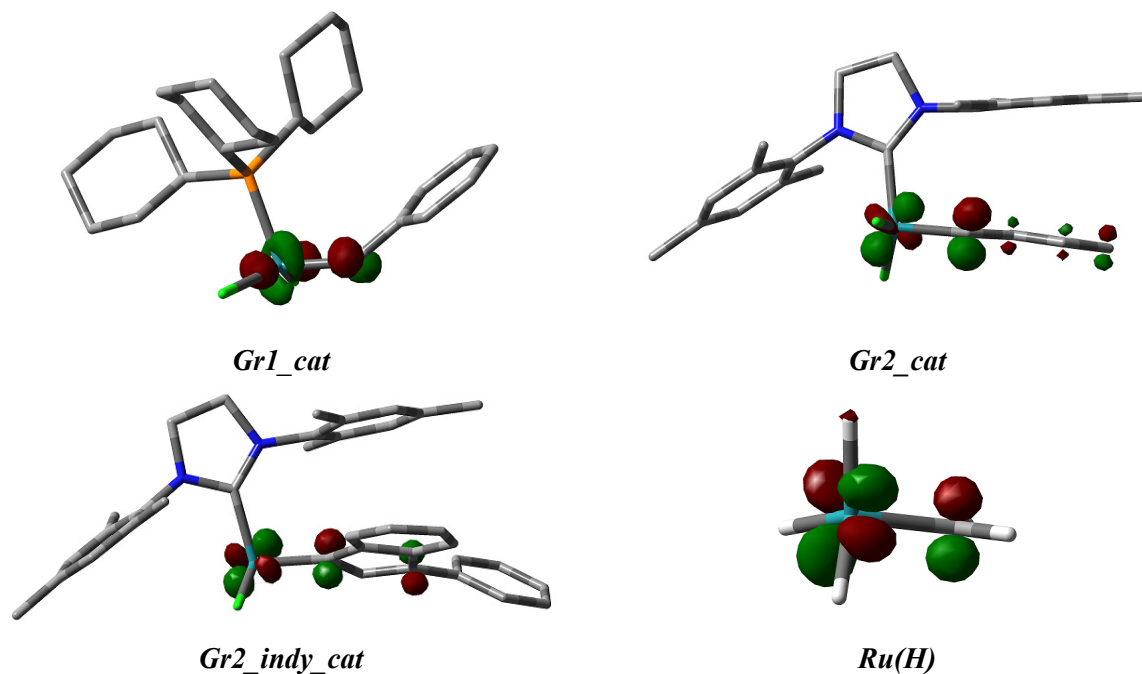
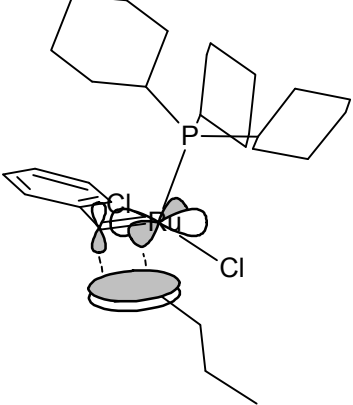
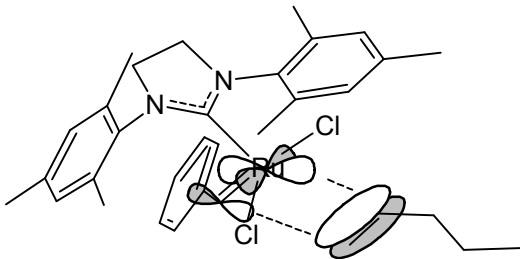
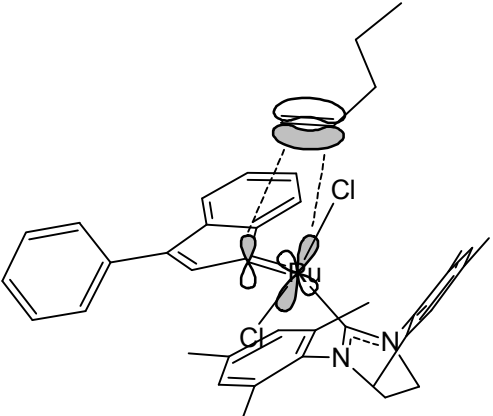
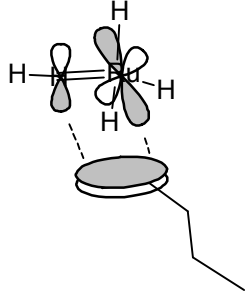


Fig. 14. LUMO surfaces with isovalue set to 0.1.

For the **Gr1\_cat**, **Gr2\_cat** and **Gr2\_indy\_cat** there is good primary overlap between the ruthenium atom and the one alkene carbon atom, with a possible secondary overlap with the carbene carbon and the other alkene carbon atom (Table 5) for the formation of the transition state. If all the ligands change to hydrogen (**Ru(H)**) there is good primary overlap between the ruthenium atom and the one alkene carbon atom, but the secondary overlap between the carbon atom of the metal carbene and the other carbon atom of the alkene is antibonding. An interesting fact is that the orientation of the AOs is the same, so the difference in activity could lie with the size of the coefficient and/or the energy of the LUMO.

**Table 5** Possible orbital overlaps indicated by dashed lines with coefficients in brackets

| <i>Gr1_cat</i> (LUMO) and alkene(HOMO)   |  | <i>Gr2_cat</i> (LUMO) and alkene(HOMO)   |  |
|--|--|--|--|
| Ru <sub>cat</sub> d <sub>xy</sub> (0.39)   | C <sub>cat</sub> p <sub>z</sub> (0.30) | Ru <sub>cat</sub> d <sub>xy</sub> (0.44)   | C <sub>cat</sub> p <sub>y</sub> (0.37) |
|   |  |    |  |
| C <sub>alk</sub> p <sub>z</sub> (0.49)   | C <sub>alk</sub> p <sub>z</sub> (0.49) | C <sub>alk</sub> p <sub>z</sub> (0.49)   | C <sub>alk</sub> p <sub>z</sub> (0.49) |
| <i>Gr2_indy_cat</i> (LUMO) and alkene(HOMO)  |  | <i>Ru(H)</i> (LUMO) and alkene(HOMO)   |  |
| Ru <sub>cat</sub> d <sub>xz</sub> (0.36)   | C <sub>cat</sub> p <sub>z</sub> (0.27) | Ru <sub>cat</sub> d <sub>yz</sub> (0.47)   | C <sub>cat</sub> p <sub>z</sub> (0.33) |
|  |  |  |  |
| C <sub>alk</sub> p <sub>z</sub> (0.49)   | C <sub>alk</sub> p <sub>z</sub> (0.49) | C <sub>alk</sub> p <sub>z</sub> (0.49)   | C <sub>alk</sub> p <sub>z</sub> (0.49) |

### 3.3 Bonding in the transition state

According to FMO theory we assumed that in the alkene metathesis mechanism the activation step is coordination of the alkene to the catalyst via the primary overlap of the HOMO of the alkene with the LUMO of the catalyst concentrated on the metal atom. This is supported in the literature [16] for the Grubbs-type carbene catalysts. In the subsequent [2+2] cycloaddition reaction, the formation of the metallacyclobutane intermediate, there is a secondary overlap of the one alkene carbon with the carbene carbon of the catalyst. To test this proposition we investigated the transition state,

before the formation of the metallacyclobutane intermediate, of the model metathesis reaction of ethene with **Gr2** as catalyst.

This was done by calculating all the MO of the transition state so that the bonding orbitals could be investigated for orbital interactions between the metal carbene and the alkene. According to the criteria used for the investigation of the MO contribution coefficients in Table 2, only the contributions of the ruthenium, the carbene carbon and the alkene carbons bigger than  $|0.2|$  were considered. It was found that the 14<sup>th</sup> bonding MO from the HOMO (HOMO-14 MO) has orbital interactions that fit the selected criteria. Molecular fragments were defined (Fig. 15) where the ruthenium atom is green, the carbene carbon is yellow, the one alkene carbon is red, the other alkene carbon is blue and the rest of the ligands are white.

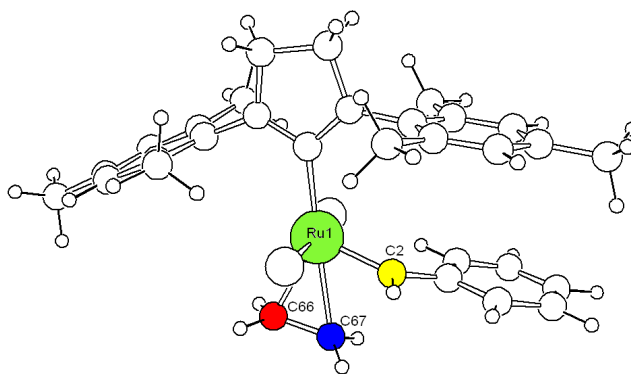
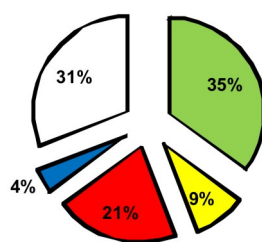


**Fig. 15.** Key to the fragmentation of the Gr2-alkene complex transition state as defined in the pie charts.

It is evident that the biggest contributions to the HOMO-14 MO come from the ruthenium atom (35%) and the one alkene carbon (21%) bonded to the ruthenium atom (Fig. 16).



*MO = HOMO-14*

**Fig. 16.** Contribution of each fragment to the molecular orbital of the Gr2-alkene complex transition state.

The biggest MO contribution coefficients (Table 6) are the Ru  $d_{xy}$  (0.39), the C66  $p_y$  (0.32) and the C2  $p_y$  (0.21). This is confirmed by the overlay of the AOs on the MO (Fig. 17).

**Table 6** |Orbital coefficients| >0.2 of the AO of Ru, the carbene carbon and the carbon atoms of ethene to the molecular orbital of the transition state

| <i>MO = HOMO-14</i> |          |             |
|---------------------|----------|-------------|
| Atom                | AO       | coefficient |
| Ru 1                | $d_{xy}$ | 0.39        |
| C 66                | $p_y$    | 0.32        |
| C 2                 | $p_y$    | 0.21        |

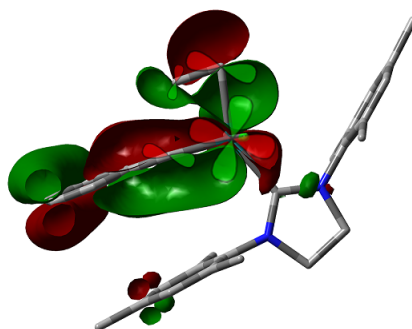


**Fig. 17.** Overlay of AO on HOMO-14 of the Gr2-alkene complex transition state.

The MO surface drawing with an isovalue set to 0.1 also supports this (Fig. 18).

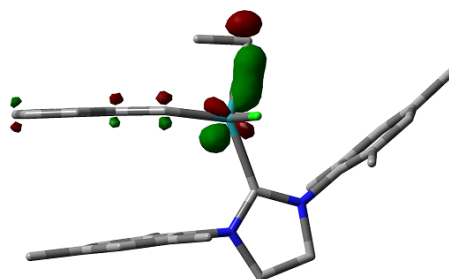


**Fig. 18.** HOMO-14 surface with isovalue set to 0.1.

The possible orbital overlap for the orientation of the AOs of each atom is shown in Table 7. This confirms the activation step of the alkene metathesis reaction where the alkene first coordinates to the metal atom.

**Table 7** Possible orbital overlaps with coefficients in brackets

| <i>Gr2_cat and alkene</i>                |  |
|--|--|
| Ru <sub>cat</sub> d <sub>xy</sub> (0.39) | C <sub>cat</sub> p <sub>y</sub> (0.21) |
|  |  |
| C <sub>alk</sub> p <sub>y</sub> (0.32)   | C <sub>alk</sub> p <sub>x</sub> (0.14) |

#### 4. Conclusion

The frontier orbital interaction of the catalyst activation step was found to be between the HOMO of the alkene and the LUMO of the catalyst for all four types of metal carbenes. The AO coefficient contributions of each fragment to the LUMO of the catalyst effectively portray the observed mechanistic pathways followed by the four types of metal carbenes. The change in percentage contribution of the metal atoms in the **W(Tol)**, **Tebbe** reagent and **Gr2** metal carbenes, confirms the importance of the catalyst initiation step in the dissociative mechanism. The value of the atomic orbital coefficients confirms the metal or carbon as the probable site for an alkene

coordination. The orientation of the alkene and the accessibility to the metal atom as well as the orientation of the d-orbitals have an effect on the possible overlap of the frontier orbitals. This gives a further insight into the difference in reactivity of the catalysts. Furthermore, the ligands directly bonded to the metal and the carbene carbon have an influence on the LUMO. Interestingly the orientation of the AOs stayed the same, but the size of the coefficient and/or the energy of the LUMO changed upon changing the ligands. Thus, the orientation and AO coefficients of the LUMO of the metal carbenes have a potential to be used as chemical reactivity indicators for the alkene metathesis activation step and subsequent [2+2] cycloaddition reaction for the formation of the metallacyclobutane intermediate.

## References

- [1] A. Hoveyda, A. Zhugralin, *Nature* 450 (2007) 243.
- [2] P. Ahlberg, Development of the metathesis method in organic synthesis, Advanced information on the Nobel Prize in Chemistry 2005. [http://nobelprize.org/nobel\\_prizes/chemistry/laureates/2005/-chemadv05.pdf](http://nobelprize.org/nobel_prizes/chemistry/laureates/2005/-chemadv05.pdf). Accessed 7 March 2008.
- [3] K.H. Dötz, H. Fischer, P. Hofmann, F.R. Kreissl, U. Schubert, K. Weiss, Transition metal carbene complexes. Verlag Chemie GmbH, Weinheim, 1983.
- [4] K.J. Ivin, Olefin metathesis. Academic Press Inc, London, 1983.
- [5] R.H. Grubbs, T.M. Trnka, M.S. Sanford, Transition Metal-Carbene Complexes in Olefin Metathesis and Related Reactions, in: H. Kurosawa, A. Yamamoto, (Eds.), Current Methods in Inorganic Chemistry: Fundamentals of Molecular Catalysis, Vol. 3. Elsevier, Amsterdam, 2003.
- [6] R.H. Grubbs, (Ed.), Handbook of metathesis, Vol. 1. Wiley-VCH, Weinheim, 2003.
- [7] V. Dragutan, I. Dragutan, A.T. Balaban, *Platinum Met. Rev.* 50 (2006) 35.
- [8] R.T. Morrison, R.N. Boyd, Organic chemistry, sixth ed. Prentice Hall International, Inc, New Jersey, 1992.
- [9] T.H. Upton, A.K. Rappé, *J. Am. Chem. Soc.* 107 (1985) 1206.

- [10] F. Mathey, A. Sevin, *Molecular Chemistry of the Transition Elements – An Introductory Course*. Wiley, Chichester, 1996.
- [11] T.J. Katz, T.H. Ho, N.Y. Shih, Y.C. Ying, V.J. Stuart, *J. Am. Chem. Soc.* 106 (1984) 2659.
- [12] F.N. Tebbe, G.W. Parshall, G.S. Reddy, *J. Am. Chem. Soc.* 100 (1978) 3611.
- [13] S.T. Nguyen, L.K. Johnson, R.H. Grubbs, *J. Am. Chem. Soc.* 114 (1992) 3974.
- [14] R.R. Schrock, J.S. Murdzek, G.C. Bazan, J. Robbins, M. DiMare, M. O'Regan, *J. Am. Chem. Soc.* 112 (1990) 3875.
- [15] G. Occhipinti, V.R. Jensen, *Organometallics* 30 (2011) 3522.
- [16] M. Tlenkopatchev, S. Fomine, *J. Organomet. Chem.* 630 (2001) 157.
- [17] O. Eisenstein, R. Hoffman, *J. Am. Chem. Soc.* 103 (1981) 5582.
- [18] C.H. Suresh, N. Koga, *Organometallics* 23 (2004) 76.
- [19] S.F. Vyboishchikov, M. Bühl, W. Thiel, *Chem. Eur. J.* 8 (2002) 3962.
- [20] B.F. Straub, *Angew. Chem. Int. Ed.* 44 (2005) 5974.
- [21] R.L. Lord, H. Wang, M. Vieweger, M. Baik, *J. Organomet. Chem.* 691 (2006) 5505.
- [22] I. Fernández, N. Lugan, G. Lavigne, *Organometallics* 31 (2012) 1155.
- [23] H. Jacobsen, *Dalton Trans.* 2006, 2214.
- [24] C. Adlhart, P. Chen, *J. Am. Chem. Soc.* 126 (2004) 3496.
- [25] S. Fomine, S.M. Vargas, M.A. Tlenkopatchev, *Organometallics* 22 (2003) 93.
- [26] F. Bernardi, A. Bottoni, G.P. Miscione, *Organometallics* 22 (2003) 940.
- [27] W. Janse van Rensburg, P.J. Steynberg, W.H. Meyer, M.M. Kirk, G.S. Forman, *J. Am. Chem. Soc.* 126 (2004) 14332.
- [28] J.L. Lippstreu, B.F. Straub, *J. Am. Chem. Soc.* 127 (2005) 7444.
- [29] W.A. Goddard III, D. Benitez, *J. Am. Chem. Soc.* 127 (2005) 12218.
- [30] S. Fomine, J.V. Ortega, M.A. Tlenkopatchev, *J. Mol. Cat. A* 236 (2005) 156.
- [31] S. Fomine, J.V. Ortega, M.A. Tlenkopatchev, *Organometallics* 24 (2005) 5696.
- [32] M. Jordaan, P. Van Helden, C.G.C.E. Van Sittert, H.C.M. Vosloo, *J. Mol. Cat. A* 254 (2006) 145.
- [33] I.T. Sabbagh, P.T. Kaye, *J. Mol. Struct.: THEOCHEM* 763 (2006) 37.

- [34] W. Janse van Rensburg, P.J. Steynberg, M.M. Kirk, W.H. Meyer, G.S. Forman, *J. Organomet. Chem.* 691 (2006) 5312.
- [35] F.T.I. Marx, J.H.L. Jordaan, H.C.M. Vosloo, *J. Mol. Model.* 15 (2009) 1371.
- [36] M.A. Tlenkopatchev, S.M. Vargas, S. Fomine, *Tetrahedron* 58 (2002) 4817.
- [37] E. Folga, T. Ziegler, *Organometallics* 12 (1993) 325.
- [38] H.H. Fox, M.H. Schofield, R.R. Schrock, *Organometallics* 13 (1994) 2804.
- [39] C.P. Casey, H.E. Tuinstra, M.C. Saeman, *J. Am. Chem. Soc.* 98 (1976) 608.
- [40] J.P. Morgan, R.H. Grubbs, *Org. Lett.* 2 (2000) 3153.
- [41] C.P. Casey, A.J. Shusterman, *J. Mol. Catal.* 8 (1980) 1.
- [42] L.J. Bosco, K.C. Ott, R.H. Grubbs, *J. Am. Chem. Soc.* 104 (1982) 7491.
- [43] E.L. Dias, S.T. Nguyen, R.H. Grubbs, *J. Am. Chem. Soc.* 119 (1997) 3887.
- [44] R.R. Schrock, A.H. Hoveyda, *Angew. Chem. Int. Ed.* 42 (2003) 4592.
- [45] R.R. Schrock, *Chem. Rev.* 109 (2009) 3211.
- [46] Accelrys Software Inc, Materials Studio Modeling Environment, Release 5.0.0.0. San Diego, Accelrys Software Inc, 2009.
- [47] M.J. Frisch, G.W. Trucks, H.B. Schlegel *et al.*, Gaussian 03, Revision B.03. Gaussian Inc, Pittsburgh PA, 2003.
- [48] S. Leonid, Chemissian Version 2.000, 2005-2011.
- [49] R.D. II, T. Keith, J. Millam, K. Eppinnett, L.W. Hovell, R. Gilliland, GaussView 3.09. Gaussian Inc, Pittsburgh PA, 2003.
- [50] I.A. Guzei, M. Wendt, Program Solid-G. UW-Madison, WI, USA, 2004.
- [51] (a) I. Fleming, *Frontier Orbitals and Organic Chemical Reactions*. WILEY, Chichester, 1976.; (b) I. Fleming, *Molecular Orbitals and Organic Chemical Reactions*, Reference Ed. WILEY, Chichester, 2010.
- [52] F. Jensen, *Introduction to Computational Chemistry*. John Wiley & Sons Inc, Chichester, 2007.
- [53] J.I. Du Toit, A modelling investigation into the mechanism of the homogeneous alkene metathesis reaction, NWU (Potchefstroom), (M.Sc. – dissertation), 2009. URL: <http://hdl.handle.net/10394/4408>.
- [54] T.J. Katz, S.J. Lee, N. Acton, *Tetrahedron Lett.* 17 (1976) 4247.
- [55] T.J. Katz, W.H. Hersh, *Tetrahedron Lett.* 18 (1977) 585



- [56] T.J. Katz, N. Acton, *Tetrahedron Lett.* 17 (1976) 4251.
- [57] C.P. Casey, T.J. Burkhardt, *J. Am. Chem. Soc.* 96 (1974) 7808.
- [58] C.P. Casey, L.D. Albin, T.J. Burkhardt, *J. Am. Chem. Soc.* 99 (1977) 2533.
- [59] C.P. Casey, S.W. Polichnowski, *J. Am. Chem. Soc.* 99 (1977) 6097.
- [60] C.P. Casey, S.W. Polichnowski, A.J. Shusterman, C.R. Jones, *J. Am. Chem. Soc.* 101 (1979) 7282.
- [61] F. Boeda, X. Bantreil, H. Clavier, S.P. Nolan, *Adv. Synth. Catal.* 350 (2008) 2959.